Measurements of temperature scaling laws in an optically dense magneto-optical trap

Andrejs Vorozcovs, Matthew Weel, Scott Beattie, Saviour Cauchi, and A. Kumarakrishnan

Department of Physics and Astronomy, York University, Toronto ON M3J 1P3, Canada

Received September 23, 2004; accepted November 22, 2004

We have studied the temperature scaling laws for the conditions under which a cloud of trapped ^{85}Rb atoms in the σ^+/σ^- configuration makes the transition from the temperature-limited regime to the multiple-scattering regime. Our experimental technique for measuring temperature relies on measuring the ballistic expansion of the cloud after turning off the confining forces and imaging the cloud size as a function of time with two CCD cameras. In the transition regime, the temperature T is shown to depend on the number of atoms N and the peak density n as $(T-T_o)\propto N^{1/3}$ and as $(T-T_o)\propto n^{2/3}$, in a manner consistent with theoretical predictions. Here T_o is defined as the equilibrium temperature of a low-density optical molasses. In the multiple-scattering regime we find that $T\propto\Omega^2/(\delta\Gamma)$, where Ω and δ are the Rabi frequency and the detuning of the trapping laser, respectively, and Γ is the natural linewidth of the cycling transition. We have also measured the ratio of temperatures along the axial and radial directions of the magnetic field gradient coils and find that the temperature is isotropic only if the intensities of the three orthogonal trapping beams are equal, and that the ratio is generally independent of trapping laser intensity and magnetic field gradient. Finally we demonstrate a measurement of the gravitational acceleration precise to $\approx$0.1% by tracking the center of the cloud during ballistic expansion.

OCIS codes: 140.3320, 140.7010, 020.7010, 040.1520, 270.1670, 300.2530.

1. INTRODUCTION

It is now routinely possible to obtain samples of laser-cooled atoms with temperatures of $\approx$100 μK in magneto-optical traps (MOTs).[1,2] Although MOTs have been widely used for precision measurements[3,4] and are used as the starting point in Bose-Einstein condensation experiments,[5,6] the temperature characteristics of a MOT have not been fully understood. This is partly because atom traps of alkali atoms are multilevel atomic systems and are thus inherently complex. Control parameters, such as laser intensity, detuning, field gradient, and number of trapped atoms, can easily be adjusted to obtain laser-cooled samples in regimes that exhibit different scaling laws for the temperature, density, and cloud size. In particular the temperature is typically strongly correlated with laser intensity, but weakly correlated with the number of atoms. This behavior is related to the modification of the mechanism of polarization-gradient cooling in the presence of multiple scattering. The characteristics of these regimes have been outlined in Refs. 7–9 and explored in Refs. 10–21. All these experiments suggest that the temperature T is proportional to the laser intensity I in the absence of multiple scattering. However, in the presence of multiple scattering, the results are somewhat inconclusive. For example Refs. 17 and 19 find that the temperature scales as $N^{1/3}(I/I_{\mathrm{sat}})^{1.5}$, and Ref. 18 reports that the temperature excess due to multiple scattering $(T-T_0)$ scales as $N^{1/3}(I/I_{\mathrm{sat}})^{1.5}(\delta/\Gamma)^{-0.89}$. Although these studies confirm the dependence on the number of atoms N predicted by Refs. 8 and 9, they are not in agreement with the predicted dependence on intensity I and detuning δ. Here T_0 is defined as the equilibrium temperature of a low-density molasses for a given laser intensity and detuning, and I_{sat} is the saturation intensity for the laser cooling transition.

It is also notable that with the exception of Refs. 15, 20, and 21, most of the experimental work pertains to Cs. In addition the experiments in Rb do not seem to have explored the influence of multiple scattering in detail. All the experimental work has also relied on a single technique to measure the temperature, namely, the time of flight of cold atoms through a probe laser placed below the falling cloud.[22] Thus the temperature measurements in previous work are characteristic of a one-dimensional velocity distribution (along the vertical axis).

Since temperature scaling laws are strongly influenced by atomic level structure, we have carried out detailed studies in ^{85}Rb and compared the trends to the Cs data. We have also measured the three-dimensional velocity distribution of the cloud to improve our understanding of theoretical predictions. To measure the temperature, we studied the ballistic expansion of the cloud as a function of time. We fit the spatial profile of the cloud to a Gaussian distribution. We have combined the cloud size data with measurements of the total number of atoms (inferred from trap fluorescence) to obtain the peak density of the cloud. We were therefore in a position to measure the scaling laws for N and n in a self-consistent manner. Our results clearly show that the temperature scaling is such that $(T-T_0)\propto N^{1/3}\delta^{-1}$ and that $(T-T_0)\propto n^{2/3}\delta^{-1}$. This behavior is observed even in the regime where the MOT makes a transition from temperature-limited behavior to the multiple-scattering-dominated regime. Our results also indicate that the temperature is strongly correlated with laser intensity I in the multiple-scattering regime $(T\propto I)$.

0740-3224/05/050943-8/$15.00

In the presence of multiple scattering, we further find that the cloud radius R scales as $N^{1/3}$ and as $\approx(\mathrm{d}B/\mathrm{d}z)^{-1}$, and that the density shows a characteristic power-law dependence on the field gradient as it saturates. These trends are particular to the multiple-scattering regime. We also find that the trap has an isotropic temperature distribution only if the intensities of the three orthogonal laser beams are equal, and the anisotropy is generally insensitive to other control parameters such as laser intensity and detuning and magnetic field gradient.

For the conditions of low intensity ($I\approx I_{\mathrm{sat}}$), $(\mathrm{d}B/\mathrm{d}z)>15$ G/cm, and $\delta>\Gamma$, we observe evidence for two-component spatial distributions as in Ref. 7. Since the temperature measurements reported here pertain to the multiple-scattering regime for which the spatial profiles are Gaussian, we are careful to avoid making the transition to the two-component regime.

We also demonstrate a measurement of the gravitational acceleration g precise to $\approx 0.1\%$ by tracking the center of the falling cloud. We discuss how this measurement can be used to infer the population distribution in the magnetic sublevels of the ground state of the cycling transition.

The rest of the paper is organized as follows. Section 2 is a discussion of the theoretical background pertaining to the temperature-limited and multiple-scattering regimes. Section 3 describes the experimental technique, and section 4 contains a discussion of the results.

2. THEORETICAL BACKGROUND

For a multilevel atomic system such as ^{85}Rb, the temperature is determined by polarization-gradient cooling.[23] In the absence of multiple scattering the cloud temperature can be described as[24]

$$\frac{k_{\mathrm{B}}T}{\hbar\Gamma}=(C_{\sigma^+\sigma^-})\frac{\Omega^2}{|\delta|\Gamma}+C_0, \tag{1}$$

where Ω^2/δ is the Stark shift given in terms of the Rabi frequency Ω and detuning δ, and $C_{\sigma^+\sigma^-}$ and C_0 are constants dependent only on the atomic level structure. The cloud temperature can also be expressed as $k_{\mathrm{B}}T=D/\alpha$, where D is the diffusion coefficient and α is the friction parameter. The polarization-gradient cooling mechanism is strongly modified in the presence of multiple scattering (which affects both D and α).

The first calculations—reported in Refs. 8 and 12 applied to a two-level atomic system—showed the influence of reradiated photons on the diffusion coefficient for an optically thick sample with constant density. In Ref. 8 the extra contribution due to multiple scattering was found to be proportional to the optical thickness of the cloud, and the diffusion coefficient was shown to vary as $N^{1/3}n^{2/3}$. This treatment assumed that the spring constant is independent of density, an assumption that is not valid if the cloud temperature is determined by polarization-gradient cooling.

Refined calculations were reported for the lin–perp–lin configuration in Ref. 9 in the far-field limit, assuming that atoms are separated by $r\gg\lambda$ and that the interaction is given by the $1/r$ potential between two excited atoms. A master equation was derived describing the influence of a rescattered background field on a single atom. This calculation applies specifically to multilevel atoms that are cooled by the mechanism of polarization-gradient cooling. In the low-intensity, large-detuning limit it was found that even a small background field due to multiple scattering could affect polarization-gradient cooling. The number of reabsorbed photons was found to scale as $N^{1/3}n^{2/3}$. The friction parameter was shown to decrease faster than the diffusion coefficient as a function of N so that the temperature increase due to multiple scattering scales as $N^{1/3}$ and δ^{-3}. Similar results were obtained for the σ^+/σ^- configuration. The predicted N dependence was verified by Refs. 17 and 18.

The characteristics of various regimes in a MOT were thoroughly explored in Ref. 7. This work describes a temperature-limited regime in which the number of atoms is of the order of $\approx 10^4$. In this regime $n\propto N$, and the radius of the cloud is independent of N. It is in this regime that most studies have shown the validity of Eq. (1).[15–17]

Another characteristic of this regime is that the spring constant is proportional to the field gradient, and the radius of the cloud scales as $(\mathrm{d}B/\mathrm{d}z)^{-1/2}$, where $(\mathrm{d}B/\mathrm{d}z)$ is the magnetic field gradient along the axial direction defined by the gradient coils. Since $k_{\mathrm{B}}T=1/2kx^2$ it is possible to argue that the temperature should be independent of the field gradient, consistent with the results of Ref. 15.

As the number of atoms increases into the multiple-scattering regime, the density increases and then saturates and the cloud volume begins to increase. It has been proposed[7] that this effect is the true signature of the multiple-scattering regime. Although experiments reported in Refs. 17 and 18 have shown that the temperature should scale as $N^{1/3}$ in the regime in which the density saturates, the arguments of Refs. 7 and 8 suggest that the temperature should scale as $N^{1/3}$ and as $n^{2/3}$ even as the cloud makes the transition from the temperature-limited regime to the multiple-scattering regime.

The results of Ref. 7 also established that the spatial profile of the cloud is described by a Gaussian distribution in both temperature-limited and multiple-scattering regimes. However, these findings contradict earlier measurements,[25] which showed uniform spatial distributions in the multiple-scattering regime. However, predictions for the dependence of peak density on δ and Ω derived in Ref. 7 and earlier in Ref. 12 have not been consistent with experiments.[7,20]

Ref. 7 also identifies a two-component regime of the trap. A trap containing $\approx 10^8$ atoms operating in the multiple-scattering regime can make a transition to the two-component regime in the presence of large field gradients and large detunings. This regime is characterized by the presence of an inner cloud within which polarization-gradient cooling occurs and an outer cloud with a temperature that is determined by Doppler cooling.

3. EXPERIMENTAL DETAILS

The basic experimental setup is shown in Fig. 1. Several laser frequencies used in the experiment are derived from a single Ti:sapphire laser. This laser is locked to an external Fabry–Perot cavity and has a linewidth of ≈1.5 MHz. The trapping laser beam is generated by an acousto-optic modulator (AOM) operating at ≈80 MHz in a dual-pass configuration.[26] A part of the Ti:sapphire light is sent to a saturated-absorption spectrometer that contains a Rb reference cell and another AOM operating at ≈80 MHz in a dual-pass configuration. The laser is locked to the $F=3 \rightarrow F=4'$ transition by means of frequency-modulation spectroscopy. This involves modulating the RF oscillator used to drive the AOM in the saturated-absorption spectrometer at a frequency of 10 kHz. The modulated signal from the reference cell is mixed down to DC to generate the dispersion line shape that is fed back to the laser. A dual-pass AOM operating at ≈80 MHz is used to generate a probe beam resonant with the $F=3 \rightarrow F=4'$ transition. Another AOM operating at ≈250 MHz is used in the undiffracted beam passing through the trapping AOM to produce an optical pumping beam resonant with the $F=3 \rightarrow F=3'$ transition. A repump beam is derived from a separate grating-stabilized-diode laser with a linewidth of ≈1 MHz. This laser is locked by saturated absorption so that the laser is resonant with the $F=2 \rightarrow F=3'$ transition. The intensity of this laser is controlled by an AOM operating at ≈40 MHz.

The MOT is loaded from Doppler-broadened Rb vapor. We typically accumulate a steady-state number of $\approx 5x10^8$ atoms in ≈300 ms with three pairs of trapping beams with a $1/e^2$ diameter of 32 mm. The beams are aligned along the axial and radial directions of the anti-Helmholtz coils. The external magnetic fields are canceled to within +/−25 mG by three pairs of Helmholtz coils.

The pulses required for controlling the AOMs, the magnetic field gradient, and the CCD cameras are provided by digital-delay generators. To measure the temperature, we record the cloud size as a function of free-expansion time. After turning off the trapping beam in ≈1 μs and the field gradient in ≈500 μs, the trapping and repumping beams are strobed for an exposure time of ≈500 μs following a variable time delay. The integrated fluorescence from the atoms during this period is recorded by two identical, analog, gray-scale CCD cameras with zoom lenses that are positioned outside the chamber and set up to image the cloud along the radial and axial symmetry directions

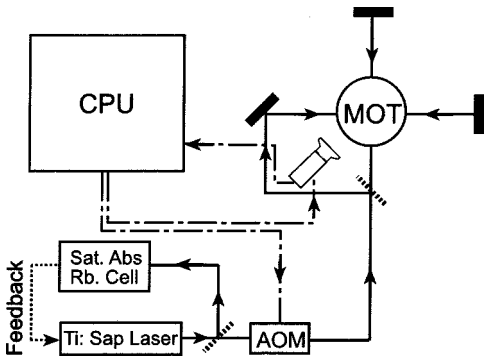

Fig. 1. Schematic of experimental setup.

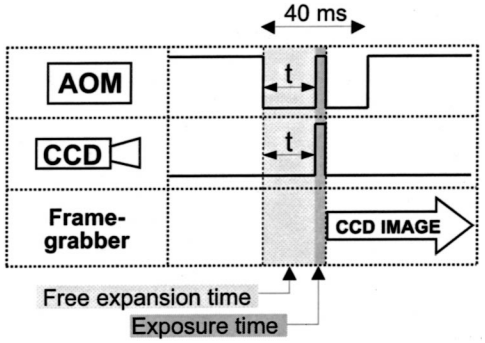

Fig. 2. CCD camera timing diagram.

of the anti-Helmholtz coils. The cameras operate in field-on-demand mode and are supplied with trigger pulses that open and close their electronic shutters as shown in Fig. 2. The shutter-open (exposure) time of the cameras is equal to the width of the trigger pulse, with a lower limit of 100 μs. The video outputs of the cameras are connected to separate inputs of a frame grabber that is triggered by the same pulse as the camera shutters. The repetition rate of our experiment (2.997 Hz) is synchronized with the camera field rate (59.94 Hz) by virtue of the sensitivity of the frame grabber to the incoming field rate. The repetition rate is limited by the loading time of the trap and the image processing time.

To study the dependence of temperature on laser intensity, we loaded the trap at the selected values of field gradient, laser intensity, and detuning. To study the temperature dependence on N and n, atoms are first accumulated by loading the trap with optimal laser intensity and detuning at the required field gradient. The number of atoms is varied by changing the trap loading time. The intensity and detuning are then switched to their final values and the cloud is allowed to equilibrate for 50 ms before the temperature measurement is carried out.

For the conditions of our experiment the spatial distribution of the cloud can be modeled by a Maxwell–Boltzmann function $n(z)=n_0 \exp(-z^2/R_{Z_0}{}^2)$, where R_{Z_0} is the initial $1/e$ cloud radius along the z direction. As in Refs. 27 and 28 we describe the expansion of the cloud as a function of time t by the quadrature sum of two Gaussian functions so that

$$R_Z(t) = [R_{Z_0}{}^2 + (v_0 t)^2]^{1/2}. \tag{2}$$

Here $v_0=(2k_B t/m_{Rb})^{1/2}$ is the most probable speed, k_B is Boltzmann's constant, and m_{Rb} is the atomic mass of Rb. The temperature is determined by fitting the cloud expansion to the hyperbola given by Eq. (2).

The number of atoms in the trap is obtained by imaging trap fluorescence on a photomultiplier tube. The initial peak density of the cloud is obtained by combining the photomultiplier tube and the cloud size measurements as in Ref. 29.

To determine the gravitational acceleration, the position of the cloud center is determined as a function of time with a two-dimensional Gaussian fit.

4. RESULTS AND DISCUSSION

A. Temperature Measurement

Figure 3 shows a typical plot of the radius of the expanding cloud as a function of time. A hyperbolic fit based on Eq. (2) gives a temperature of 121 μK along the axial (z) direction with a statistical uncertainty of 0.89% for T. Repeated runs for the same conditions suggest that the temperature can be determined to a precision of 1%. The temperature measurements did not exhibit any appreciable systematic effects if the variation of the camera exposure time and strobe laser intensity were limited to the range 0.5–2.0 ms and 10–60 mW/cm^2, respectively.

B. Transition from the Temperature-Limited to the Multiple-Scattering Regime

Figure 4(a) shows the peak density of the cloud as a function of the atom number for a range of magnetic field gradients. The number of atoms was varied by changing the intensity and/or detuning of the trapping laser. The results are similar to the work of Ref. 7 and show that the MOT makes a transition from the temperature-limited regime to a regime with a constant density that would be expected in the presence of multiple scattering. The trap volume increases even as the density approaches saturation as shown in Fig. 4(b). As noted in Ref. 7 this measurement represents a sensitive method of observing the presence of multiple scattering.

C. Dependence on Magnetic Field Gradient

Figure 5 shows the temperature dependence on the magnetic field gradient for a fixed laser intensity and detuning. It is well known from Ref. 7 that the density is proportional to the field gradient in the presence of multiple scattering. As the gradient increases, the density approaches its equilibrium value. The data essentially indicate that for fixed laser intensity, the change in temperature is associated with the change in the density of the cloud. Thus for $dB/dz > 1.3$ G/cm the temperature shows very little variation. As the gradient tends to zero, the vertical intercept would represent the temperature of the optical molasses. In comparison, in the absence of multiple scattering the temperature of the MOT was measured to be the same as the temperature of the optical molasses for the same laser detuning and intensity.[15,16]

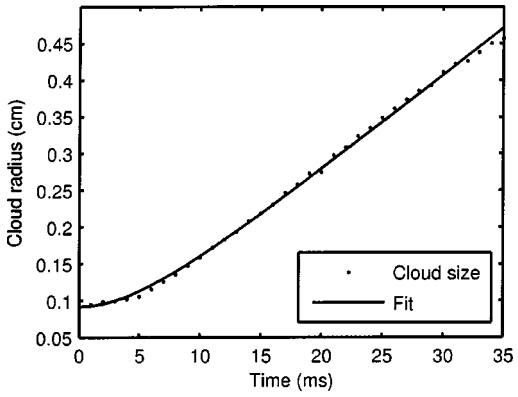

Fig. 3. Cloud radius [given by Eq. (2)] as a function of time; $T = 121 \pm 0.9$ μK, $R_{Z_0} = (9.2 \pm 0.2) \times 10^{-3}$ m, $I = 60$ mW/cm^2, $\delta = -2.0\Gamma$, $\partial B/\partial z = 1$ G/cm.

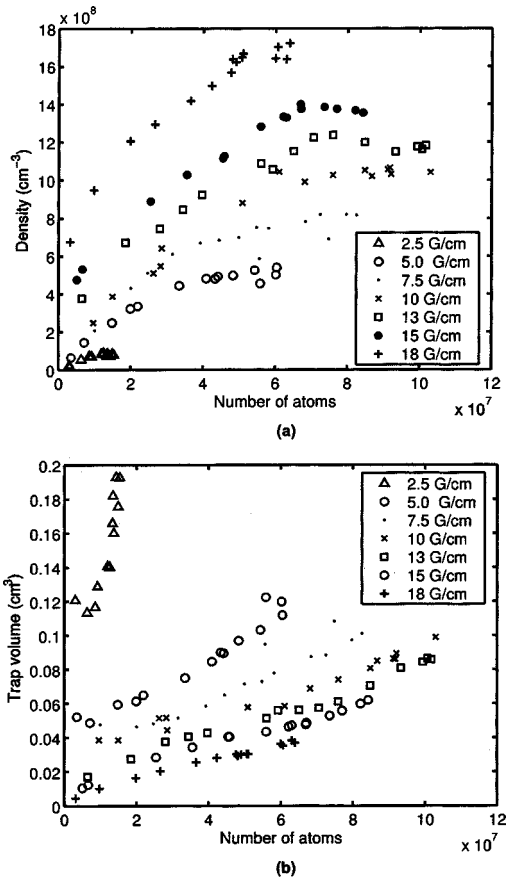

Fig. 4. (a) Peak density n and (b) trap volume V versus number of atoms N.

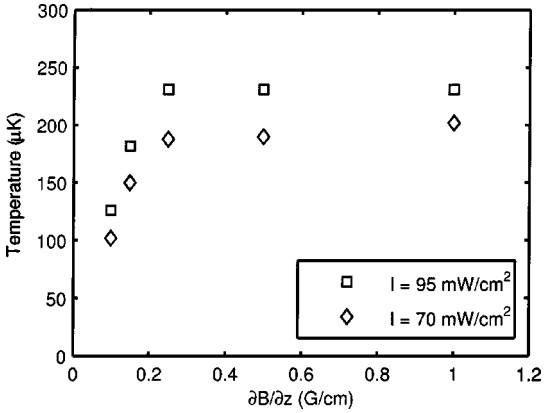

Fig. 5. Temperature versus field gradient; $\delta = -4.0\Gamma$.

In the absence of multiple scattering, the cloud radius scales as $dB/dz^{-0.5}$ and the spring constant exhibits a linear dependence on dB/dz.[15] As discussed in Section 2 it can be argued that on the basis of the equipartition theorem the MOT temperature should be independent of the field gradient, an expectation that has been experimentally confirmed.[15,16]

In contrast the results of this experiment (in the presence of multiple scattering) show that the cloud radius scales as $(dB/dz)^{-1}$ for $dB/dz = 0.1$–1.0 G/cm and a fixed laser intensity. We observe similar behavior for laser intensities in the range of 10–100 mW/cm^2.

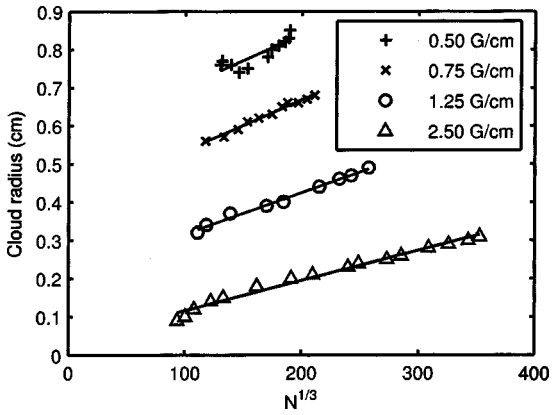

Fig. 6. Cloud radius as a function of $N^{1/3}$ for a range of field gradients; $\delta=-4.0\Gamma$.

D. Cloud Radius

Another significant result of this work is that we unambiguously observe that the radius of the cloud scales as $N^{1/3}$ in the multiple-scattering regime as predicted by Ref. 7. This scaling is observed when the density (which is proportional to field gradient) reaches its maximum value. Figure 6 shows R versus $N^{1/3}$ for a range of field gradients at a fixed detuning of -4Γ. The number of atoms was varied by changing the laser intensity. The linear dependence shows that the density n has attained its limiting value. We have also verified that at detunings closer to resonance, the peak density remains independent of the field gradient for higher values of field gradient.

E. Temperature as a Function of Intensity in the Multiple-Scattering Regime

We now discuss temperature measurements as a function of laser intensity in the presence of multiple scattering. Figure 7(a) shows temperature as a function of laser intensity for various trap laser detunings. The data were obtained with a field gradient of 2.5 G/cm and show that the temperature exhibits a strongly correlated linear dependence on laser intensity. This behavior is consistent with predictions for polarization-gradient cooling and has been observed by many groups in the absence of multiple scattering.[15,17,21] The data can also be represented on a universal plot in which the horizontal axis is the dimensionless Stark shift parameter $\Omega^2/\delta\Gamma$ as shown in Fig. 7(b). We fitted the data to straight lines represented by Eq. (1), where the slope $C_{\sigma^+\sigma^-}$ depends only on the level structure of the trapping transition and C_0 is the temperature intercept. This fit, shown as a dashed curve in Fig. 7(b), gives $C_{\sigma^+\sigma^-}=0.36\pm0.02$, and the value of this parameter was found to vary by $\approx 10\%$ over several data sets, presumably related to alignment of the trapping beams.

The solid curve is a fit to the data with $(dB/dz)=2.5$ G/cm and $\delta=-4\Gamma$ for which I was varied from 2 to 70 mW/cm^2. The fit results in $C_{\sigma^+\sigma^-}=0.65\pm0.02$. Since the temperature (in this regime) does not vary if the field gradient is increased, it is possible to compare our results with previous measurements in Rb[15] obtained in the absence of multiple scattering with $N<10^6$. The results of Ref. 15, shown as a dotted curve, give $C_{\sigma^+\sigma^-}=0.46\pm0.02$ (for $\delta=-4.14\Gamma$, $dB/dz=10$ G/cm). We attribute this difference in temperature to the presence of multiple scattering. The breakdown of polarization-gradient cooling observed in Ref. 15 at low intensities was not observed in our experiments.

Nevertheless, the universal plot in Fig. 7(b) is somewhat misleading. We find a systematic dependence for $C_{\sigma^+\sigma^-}$ on the detuning as demonstrated by two data sets in Fig. 7(c). The data in Ref. 15 also seem to show such a

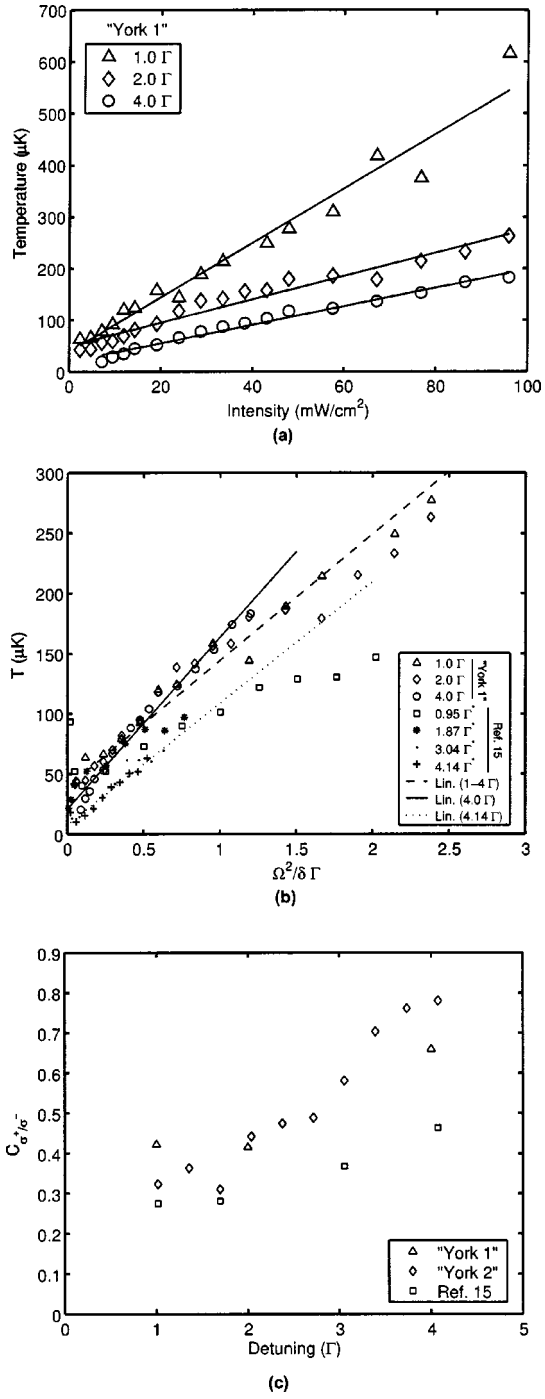

Fig. 7. (a) Temperature versus laser intensity, (b) light-shift parameter for a range of laser detunings, (c) coefficient $C_{\sigma^+\sigma^-}$ versus laser detuning δ; $\partial B/\partial z=2.5$ G/cm for our experiments and 10 G/cm for the data in Ref. 15; $I_{\mathrm{sat}}=3.24$ mW/cm^2.

trend. This trend suggests that Eq. (1) is valid only in the large detuning limit, but should nevertheless be examined in greater detail. The results of Ref. 16 suggest that such a systematic dependence is unlikely at large detunings.

F. Temperature as a Function of N in the Multiple-Scattering Regime

Since the temperature variation in Fig. 7(a) and 7(b) is strongly correlated with laser intensity, we have carried out separate experiments as discussed in Section 3 to study the temperature variation due to multiple scattering by varying N and δ independently.

Figure 8 shows the temperature variation as a function of N for a fixed field gradient, laser intensity, and a range of detunings. Here N was varied by changing the loading time of the trap. The data are well approximated by the function $T=T_0+aN^{1/3}$. We find that this scaling law applies in the range when the cloud makes a transition from the temperature-limited to the multiple-scattering regime, thus confirming the predictions of Refs. 8 and 9. The data also confirm the scaling law observed in Cs.[17,18] The intercepts in Fig. 8 represent the equivalent molasses temperature and show that $T_0 \propto \delta^m$, where $m=1.0\pm0.1$. The δ^{-1} trend is predicted by Eq. (1) and has been previously observed.[19] In contrast Ref. 17 reported $\delta^{-0.89}$.

Figure 9 shows the temperature variation as a function of peak density for a fixed field gradient and laser intensity. The data are fitted to the functional form $T=T_0+an^{2/3}$ and confirm the dependence predicted in Refs. 8 and 9. As in Fig. 8 we find that the intercepts represent the molasses temperature in a manner consistent with Eq. (1).

G. Temperature Anisotropy

We have measured the temperature anisotropy in the trap, $T_{\text{axial}}/T_{\text{radial}}$, for typical operating conditions, $\delta=2\Gamma$, as a function of laser intensity and field gradient. Figure 10(a) shows the ratio of axial to radial temperatures in the cloud in the multiple-scattering regime. The ratio is independent of total laser intensity and magnetic field gradient. This behavior suggests that the scaling laws for the temperature dependence on density and atom number should be valid for all three dimensions. We have confirmed this by analyzing axial and radial temperatures separately.

Figure 10(b) shows the cloud radius along the axial and radial symmetry axes of the magnetic field coils as a function of the intensity ratio $I_{\text{axial}}/I_{\text{radial}}$. The corresponding temperatures are shown in Fig. 10(c). These data were obtained by keeping the total trapping intensity constant and changing the relative powers of the axial and radial trapping beams by use of a half-wave plate and a polarizing beam splitter. The optimal conditions for the trap are in the vicinity of $I_{\text{axial}}/I_{\text{radial}}\approx 1.0$.

We find that the axial size decreases gradually when the fraction of light intensity along the axial direction is increased, and that the corresponding radial size increases gradually with decreasing radial intensity.

In Fig. 10(c) we see that the temperature decreases as the intensity fraction deviates from the typical operating value of ≈ 1. We attribute this behavior to a reduced amount of multiple scattering for extreme trap size ratios, which leads to a decrease in temperature. It is interesting to note that Ref. 30 also demonstrates this behavior for spatially anisotropic clouds. In Ref. 30 the focus is on exploiting the properties of multiple scattering to increase phase-space density in highly anisotropic traps.

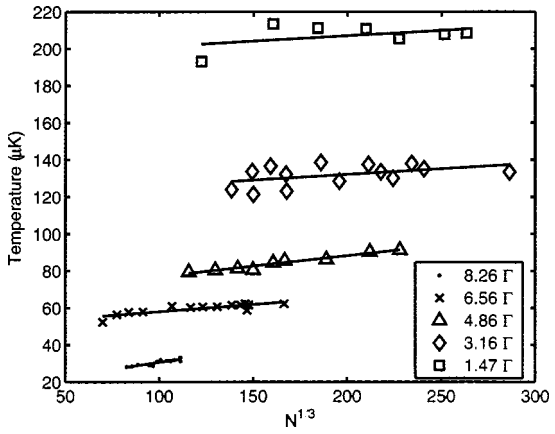

Fig. 8. Temperature versus $N^{1/3}$; $\partial B/\partial z=10$ G/cm, $I=60$ mW/cm^2.

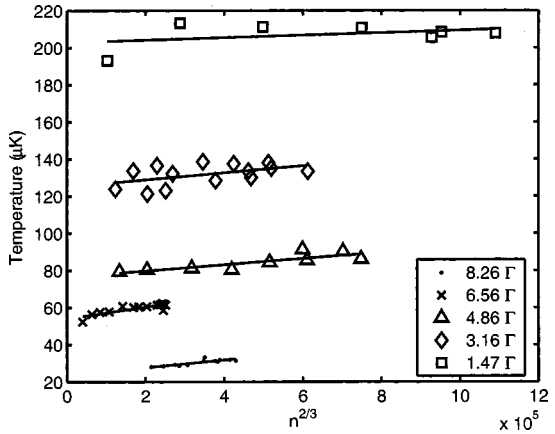

Fig. 9. Temperature T versus $n^{2/3}$; $\partial B/\partial z=10$ G/cm, $I=60$ mW/cm^2.

H. Gravity Measurements

Figure 11 shows the position of the center of the cloud as a function of time with a parabolic fit given by $z(t)=z_0+\frac{1}{2}g_{\text{eff}}t^2$. The center of the cloud is found with a two-dimensional search algorithm that uses least-squares Gaussian fits. Here z_0 is the initial position of the center of the cloud and g_{eff} is the gravitational acceleration. The statistical uncertainty in g_{eff} from the fit is 0.4% and from repeated measurements we are able to determine g_{eff} to a precision of 0.1%. The dominant systematic effect in the measurement of g_{eff} seems to be the result of misalignment of the laser beams with respect to the zero point of the magnetic field. This causes the cloud to be launched and results in fitting errors during the first 1–2 ms after trap turn-off. Other effects include the presence of eddy currents when the MOT coils are turned off and residual magnetization present in the vacuum chamber.

For typical conditions ($\delta=2\Gamma, I=50$ mW/cm$^2, N\approx 10^8$) polarization-gradient cooling has the effect of optically

pumping atoms to magnetic sublevels with larger m values.[7] We have confirmed this effect by measuring the populations of the magnetic sublevels of the $F=3$ ground state by use of absorption spectra. We have also been able to control the distribution of sublevel populations. This is carried out by turning off the trap and applying circularly polarized optical pumping pulses resonant with the $2 \rightarrow 3'$ and $3 \rightarrow 3'$ transitions in the presence of a weak quantizing magnetic field.[29] Varying the optical pumping time allows us to transfer up to $\approx 100\%$ of the atoms into the $F=3$, $m_f=3$ sublevel. After the atoms are optically pumped in the desired manner, it is possible to turn on a field gradient and measure g_{eff}. Since each magnetic sublevel has a specific acceleration due to the field gradient, it is possible to investigate if the measurement of g_{eff} could result in a simple diagnostic for determining the magnetic sublevel populations. Such experiments could prove useful for precision measurements of the atomic recoil frequency and gravitational acceleration by use of atom interferometry.[31,32]

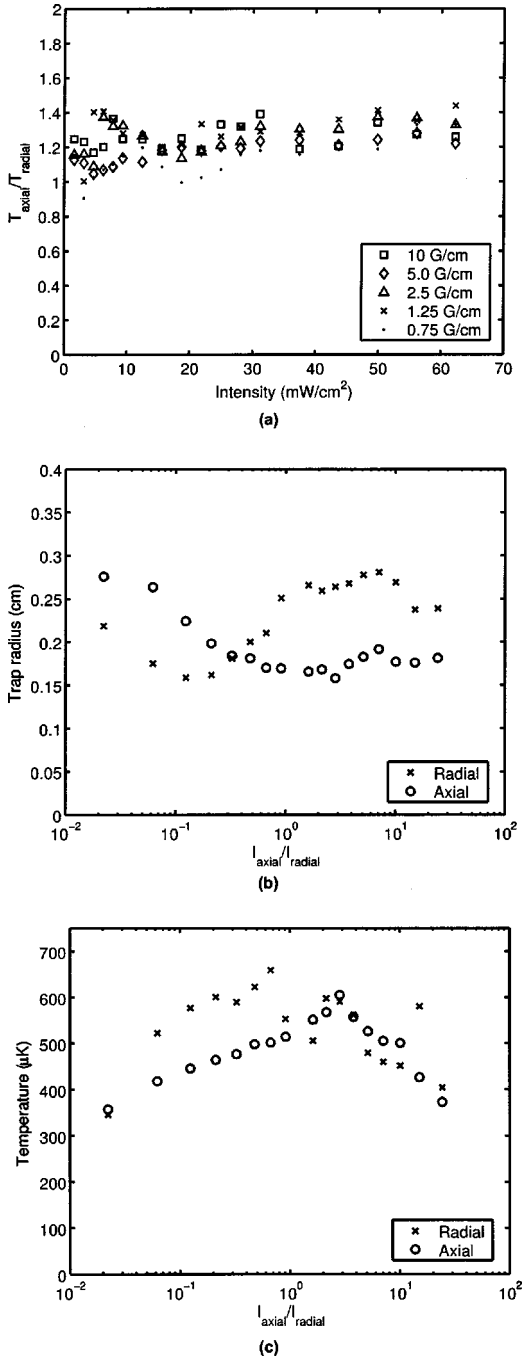

Fig. 10. (a) Ratio of radial to axial temperatures versus laser intensity for a variety of field gradients; (b) cloud radius, (c) temperature as a function of $I_{\mathrm{axial}}/I_{\mathrm{radial}}$ with $\delta=-2.0\Gamma$, $I=60$ mW/cm^2, $\partial B/\partial z = \approx 10$ G/cm.

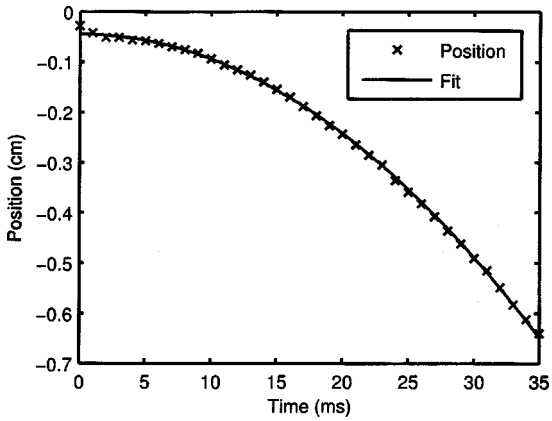

Fig. 11. Gravity measurement showing the position of cloud center as a function of time; $z_0=4.51\times10^{-4}$ m, $g_{\mathrm{eff}}=9.870\pm0.038$ m/s^2, $I=\approx 60$ mW/cm^2, $\delta=-2.0\Gamma$, $\partial B/\partial z=1.0$ G/cm.

5. CONCLUSIONS

We have verified that the mechanism of polarization-gradient cooling is valid in the multiple-scattering regime, and our results are consistent with those of Refs. 7 and 17. As in Ref. 7 we see the peak density equilibrate and the volume increase as we enter the multiple-scattering regime. We have verified the predicted dependence of the cloud size on the number of atoms in the multiple-scattering regime. We observe the $R^{1/3}$ characteristic of equilibrium density.

We have also confirmed that the temperature scales as $N^{1/3}$ in the transition region between the temperature-limited and multiple-scattering regimes. This essentially confirms the prediction of Ref. 8. The $N^{1/3}$ dependence, which was originally observed in Cs,[18] has now been confirmed in ^{85}Rb. For the first time we have confirmed the $n^{2/3}$ scaling law for the temperature by measuring the temperature, the number of atoms, and the cloud size. We note that with respect to variation in N, our results are not consistent with those of Ref. 17 or Ref. 19. The detuning dependence, however, is approximately consistent with that reported in Ref. 18.

We have also presented evidence of spatially anisotropic temperature distributions in a MOT, even for fairly typical operating conditions.

Further, we have demonstrated a convenient method of measuring by means of a CCD the acceleration due to gravity that is precise to $\approx 0.1\%$. We are investigating the applicability of this method to measuring imbalances in magnetic sublevel populations.

ACKNOWLEDGMENTS

This work was supported by Canada Foundation for Innovation, Ontario Innovation Trust, Natural Sciences and Engineering Research Council of Canada, Photonics Research Ontario, and York University.

Corresponding author A. Kumarakrishnan can be reached by e-mail at akumar@yorku.ca.

REFERENCES

1. E. L. Raab, M. Prentiss, A. Cable, S. Chu, and D. E. Pritchard, "Trapping of neutral sodium atoms with radiation pressure," Phys. Rev. Lett. **59**, 2631–2634 (1987).
2. C. Monroe, W. Swann, H. Robinson, and C. Wieman, "Very cold trapped atoms in a vapor cell," Phys. Rev. Lett. **65**, 1571–1574 (1990).
3. M. Kasevich and S. Chu, "Atomic interferometry using stimulated Raman transitions," Phys. Rev. Lett. **67**, 181–184 (1991).
4. C. W. Oates, K. R. Vogel, and J. L. Hall, "High precision linewidth measurement of laser-cooled atoms: resolution of the $Na3p^2P_{3/2}$ lifetime discrepancy," Phys. Rev. Lett. **76**, 2866–2869 (1996).
5. M. H. Anderson, J. R. Ensher, M. R. Matthews, C. E. Wieman, and E. A. Cornell, "Observation of Bose–Einstein condensation in a dilute atomic vapor," Science **269**, 198–201 (1995).
6. K. B. Davis, M. O. Mewes, M. R. Andrews, N. J. van Druten, D. S. Durfee, D. M. Kurn, and W. Ketterle, "Bose-Einstein condensation in a gas of sodium atoms," Phys. Rev. Lett. **75**, 3969–3973 (1995).
7. C. G. Townsend, N. H. Edwards, C. J. Cooper, K. P. Zetie, C. J. Foot, A. M. Steane, P. Szriftgiser, H. Perrin, and J. Dalibard, "Phase-space density in the magneto-optical trap," Phys. Rev. A **52**, 1423–1440 (1995).
8. G. Hillenbrand, C. J. Foot, and K. Burnett, "Heating due to long-range photon exchange interactions between cold atoms," Phys. Rev. A **50**, 1479–1489 (1994).
9. G. Hillenbrand, K. Burnett, and C. Foot, "Effect of scattered radiation on sub-Doppler cooling," Phys. Rev. A **52**, 4763–4786 (1995).
10. K. Lindquist, M. Stephens, and C. Wieman, "Experimental and theoretical study of the vapor-cell Zeeman optical trap," Phys. Rev. A **46**, 4082–4090 (1992).
11. K. E. Gibble, S. Kasapi, and S. Chu, "Improved magneto-optic trapping in a vapor cell," Opt. Lett. **17**, 526–528 (1992).
12. T. Walker, D. Sesko, and C. Wieman, "Collective behavior of optically trapped neutral atoms," Phys. Rev. Lett. **64**, 408–411 (1990).
13. A. M. Steane and C. J. Foot, "Laser cooling below the Doppler limit in a magneto-optical trap," Europhys. Lett. **14**, 231–236 (1991).
14. A. Hope, D. Haubrich, G. Muller, W. G. Kaenders, and D. Meschede, "Neutral cesium atoms in strong magnetic-quadrupole fields at sub-Doppler temperatures," Europhys. Lett. **22**, 669–674 (1993).
15. C. D. Wallace, T. P. Dinneen, K. Y. N. Tan, A. Kumarakrishnan, P. L. Gould, and J. Javanainen, "Measurements of temperature and spring constant in a magneto-optical trap," J. Opt. Soc. Am. B **11**, 703–711 (1994).
16. C. Salomon, J. Dalibard, W. D. Phillips, A. Clairon, and S. Guellatti, "Laser cooling of cesium atoms below 3 μK," Europhys. Lett. **12**, 683–688 (1990).
17. M. Drewsen, Ph. Laurent, A. Nadir, G. Santarelli, A. Clairon, Y. Castin, D. Grison, and C. Salomon, "Investigation of sub-Doppler cooling effects in a cesium magneto-optical trap," Appl. Phys. B: Lasers Opt. **59**, 283–298 (1994).
18. C. J. Cooper, G. Hillenbrand, J. Rink, C. G. Townsend, K. Zetie, and C. J. Foot, "The temperature of atoms in a magneto-optical trap," Europhys. Lett. **28**, 397–402 (1994).
19. S. Grego, M. Colla, A. Fioretti, J. H. Muller, P. Verkerk, and E. Arimondo, "A cesium magneto-optical trap for cold collisions studies," Opt. Commun. **132**, 519–526 (1996).
20. C. Gabbanini, A. Evangelista, S. Gozzini, A. Lucchesini, A. Fioretti, J. H. Muller, M. Colla, and E. Arimondo, "Scaling laws in magneto-optical traps," Europhys. Lett. **37**, 251–256 (1997).
21. C. Gerz, T. W. Hodapp, P. Jessen, K. M. Jones, W. D. Phillips, C. I. Westbrook, and K. Molmer, "The temperature of optical molasses for two different atomic angular momenta," Europhys. Lett. **21**, 661–666 (1993).
22. P. D. Lett, W. D. Phillips, S. L. Rolston, C. E. Tanner, R. N. Watts, and C. I. Westbrook, "Optical molasses," J. Opt. Soc. Am. B **6**, 2084–2107 (1989).
23. J. Dalibard and C. Cohen-Tannoudji, "Laser cooling below the Doppler limit by polarization gradients: simple theoretical models," J. Opt. Soc. Am. B **6**, 2023–2045 (1989).
24. Y. Castin and K. Molmer, "Monte Carlo wave-function analysis of 3D optical molasses," Phys. Rev. Lett. **74**, 3772–3775 (1995).
25. D. W. Sesko, T. J. Walker, and C. E. Wieman, "Behavior of neutral atoms in a spontaneous force trap," J. Opt. Soc. Am. B **8**, 946–958 (1991).
26. G. Spirou, I. Yavin, M. Weel, A. Vorozcovs, A. Kumarakrishnan, P. R. Battle, and R. C. Swanson, "A high-speed-modulated retro-reflector for lasers using an acousto-optic modulator," Can. J. Phys. **81**, 625–638 (2003).
27. D. S. Weiss, E. Riis, Y. Shevy, P. J. Ungar, and S. Chu, "Optical molasses and multilevel atoms: experiment," J. Opt. Soc. Am. B **6**, 2072–2083 (1989).
28. D. Guery-Odelin, J. Soeding, P. Desbiolles, and Jean Dalibard, "Strong evaporative cooling of a trapped cesium gas," Opt. Express **2**, 323–329 (1998).
29. S. Cauchi, A. Vorozcovs, M. Weel, S. Beattie, O. Gagnon, and A. Kumarakrishnan, "Absorption spectroscopy of trapped rubidium atoms," Can. J. Phys. **82**, 905–916 (2004).
30. M. Vengalattore, R. S. Conroy, and M. G. Prentiss, "Enhancement of phase space density by increasing trap anisotropy in a magneto-optical trap with a large number of atoms," Phys. Rev. Lett. **92**, 183001 (2004).
31. M. Weel and A. Kumarakrishnan, "Observation of ground-state Ramsey fringes," Phys. Rev. A **67**, 061602(R) (2003).
32. M. Weel, S. Beattie, I. Chan, E. Rotberg, A. Vorozcovs, and A. Kumarakrishnan, "A precision measurement of atomic recoil using grating echoes," Phys. Rev. Lett., submitted for publication.